Original articles / Оригинальные статьи
https://doi.org/10.47093/2218-7332.2022.338.06

Lifetime imaging of the discrete nanophosphors in biological systems

Artyom O. Zvyagintcev[1], Andrey V. Yudintsev[2], Alireza Maleki[3], Vladimir A. Vodeneev[2], Andrei V. Zvyagin[2,3,✉]

[1] Federal Scientific Research Centre "Crystallography and Photonics" of Russian Academy of Sciences
59, Leninsky Prospekt, Moscow, 119333, Russia
[2] Lobachevsky Nizhny Novgorod State University
23, bld. 2, Prospekt Gagarina, Nizhny Novgorod, 603022, Russia
[3] Macquarie University
Balaclava Road, North Ryde NSW 2109, Sydney, Australia

Abstract

The aim. Demonstrate a novel modality of laser-scanning multiphoton microscopy suitable for rapid acquisition of images of samples labelled with phosphorescent materials characterised by long emission lifetime measured in microseconds. The reported microscopy represents an advancement over the existing laser-scanning modalities, where the acquisition of images of phosphorescent materials takes unpractically long time.

Materials and methods. The reported method is based on rapid scanning of the focussed excitation beam across a sample while continuously recording the photoluminescent (PL) signal. The resultant images of discrete phosphorescent nanoparticles appeared blurred. The diffraction-limited image was reconstructed by using a deconvolution algorithm, where the PL lifetime was the key input parameter. To test the method, two types of upconversion nanoparticles (UCNP) were synthesised, $NaYF_4$:Yb^3+:Er^{3+}/$NaYF_4$ (E-UCNP), β-$NaYF_4$:Yb^{3+}, Tm^{3+}/$NaYF_4$ (T-UCNP) and used to test a possibility of demultiplexing the two types of UCNPs *ex vivo* taken up in the mouse liver.

Results. The resultant images of E-UCNP, T-UCNP on the background of the liver were fully reconstructed and exhibited the enhanced signal-to-noise ratio. Besides, the method allowed rapid (at the scale of seconds) acquisition of the UCNP PL lifetime and clear discrimination of the two types of UCNPs.

Conclusion. We demonstrated a new approach for rapid PL image acquisition of samples containing PL materials, such as biological specimens labelled with discrete UCNPs. Blurred images were shown to be reconstructed at the post-processing stage by applying a deconvolution procedure. This enabled demonstration of multiplexing/demultiplexing using lifetime imaging mode, where the lifetime was engineered by the UCNP synthesis and reconstructed during multiphoton image acquisition using the deconvolution algorithm. The power of this method was demonstrated by the identification of two types of UCNPs accumulated in the liver of a laboratory animal. We believe that the demonstrated method can be useful for rapid lifetime imaging where several molecular specific labelling agents are required.

Keywords: biophotonics; lifetime imaging; phosphorous materials; upconversion nanoparticles photoluminescence; multiphoton microscopy

MeSH terms:
INTRAVITAL MICROSCOPY
NANOPARTICLES
MICROSCOPY, CONFOCAL
PHOSPHORUS COMPOUNDS
DIAGNOSTIC USES OF CHEMICALS

For citation: Zvyagintcev A.O., Yudintsev A.V., Maleki A., Vodeneev V.A., Zvyagin A.V. Lifetime imaging of the discrete nanophosphors in biological systems. Sechenov Medical Journal. 2022; 13(1): 43–54. https://doi.org/10.47093/2218-7332.2022.338.06

CONTACT INFORMATION:
Andrei V. Zvyagin, Dr. of Sci. (Physics and Mathematics), Biomedical Physics Group, Head Faculty of Science and Engineering Macquarie University, Sydney, Australia
Address: Balaclava Road, North Ryde NSW 2109, Sydney, Australia
Tel.: +7 (909) 924 91 16
E-mail: andrei.zvyagin@mq.edu.au

Conflict of interests. The authors declare that there is no conflict of interest.
Financial support. The authors wish to acknowledge financial support from the Russian Foundation of Basic Research (RFBR), grant No 20-04-00182.

Received: 26.08.2021
Accepted: 05.10.2021
Published Online: 10.02.2022
Date of publication: 23.06.2022

УДК 616-076:57.086.3

Визуализация дискретных нанофосфоров в биологических системах с учетом времени жизни флуоресценции

А.О. Звягинцев[1], А.В. Юдинцев[2], А. Макели[3], В.А. Воденеев[2], А.В. Звягин[2,3]✉
[1] ФНИЦ «Кристаллография и фотоника» Российской академии наук
Ленинский проспект, д. 59, г. Москва, 119333, Россия
[2] ФГАУ ВО «Национальный исследовательский Нижегородский государственный университет им. Н.И. Лобачевского» (ННГУ)
пр. Гагарина, д. 23, корп. 2, Нижний Новгород, 603022, Россия
[3] Университет Маккуори
Балаклавская дорога, Норт-Райд, Новый Южный Уэльс, Сидней, 2109, Австралия

Аннотация

Цель. Продемонстрировать новый метод лазерной сканирующей многофотонной микроскопии, подходящий для быстрого получения изображений образцов, меченных фосфоресцирующими материалами, характеризующихся длительным временем жизни излучения, измеряемым в микросекундах. Представленная микроскопия представляет собой прогресс по сравнению с существующими методами лазерного сканирования, в которых получение изображений фосфоресцирующих материалов занимает непрактично долгое время.

Материал и методы. Описанный метод основан на быстром сканировании сфокусированного луча возбуждения по образцу при непрерывной регистрации фотолюминесцентного (PL) сигнала. Полученные изображения дискретных фосфоресцирующих наночастиц выглядели размытыми. Изображение с дифракционным разрешением было восстановлено с использованием алгоритма деконволюции, где время жизни PL было ключевым входным параметром. Для тестирования метода были синтезированы два типа апконверсионных частиц (UCNP): $NaYF_4$:Yb^{3+}:Er^{3+}/$NaYF_4$ (E-UCNP), β-$NaYF_4$:Yb^{3+},Tm^{3+}/$NaYF_4$ (T-UCNP) и использованы для проверки возможности демультиплексирования двух типов UCNP *ex vivo*, доставленных в печень лабораторной мыши.

Результаты. Полученные изображения E-UCNP, T-UCNP на фоне печени были полностью реконструированы и показали улучшенное отношение сигнал/шум. Кроме того, метод позволял быстро (в масштабе секунд) получать время жизни PL UCNP и четко различать два типа UCNP.

Заключение. Мы продемонстрировали новый подход для быстрого получения изображений PL-образцов, содержащих флуоресцирующие вещества, например биологических образцов, меченных дискретными UCNP. Было показано, что размытые изображения восстанавливаются на этапе постобработки путем применения процедуры деконволюции. Это позволило продемонстрировать мультиплексирование/демультиплексирование в режиме визуализации времени жизни, где время жизни определялось синтезом UCNP и восстанавливалось во время получения многофотонного изображения с помощью алгоритма деконволюции. Возможности этого метода были продемонстрированы на примере идентификации двух типов UCNP, накопленных в печени лабораторного животного. Мы считаем, что продемонстрированный метод может быть полезен для быстрой прижизненной визуализации, когда требуется несколько молекулярно-специфических меченых агентов.

Ключевые слова: биофотоника; прижизненная визуализация; фосфорсодержащие материалы; фотолюминесценция наночастиц с восходящей конверсией; многофотонная микроскопия
Рубрики MeSH:
ПРИЖИЗНЕННАЯ МИКРОСКОПИЯ
НАНОЧАСТИЦЫ
МИКРОСКОПИЯ КОНФОКАЛЬНАЯ
ФОСФОРА СОЕДИНЕНИЯ
ДИАГНОСТИЧЕСКОЕ ПРИМЕНЕНИЕ ХИМИЧЕСКИХ ВЕЩЕСТВ
Для цитирования: Звягинцев А.О., Юдинцев А.В., Малеки А., Воденеев В.А., Звягин А.В. Визуализация дискретных нанофосфоров в биологических системах с учетом времени жизни флуоресценции. Сеченовский вестник. 2022; 13(1): 43–54. https://doi.org/10.47093/2218-7332.2022.338.06

КОНТАКТНАЯ ИНФОРМАЦИЯ:
Андрей Васильевич Звягин, д-р физ.-мат. наук, группа биомедицинской физики; руководитель факультета науки и техники Университета Маккуори.
Адрес: Балаклавская дорога, Норт-Райд, Новый Южный Уэльс, Сидней, 2109, Австралия.
Тел.: +7 (909) 924 91 16
E-mail: andrei.zvyagin@mq.edu.au

Конфликт интересов. Авторы заявляют об отсутствии конфликта интересов.
Финансирование. Авторы выражают благодарность за финансовую поддержку Российскому фонду фундаментальных исследований (РФФИ), грант № 20-04-00182

Поступила: 26.08.2021
Принята: 05.10.2021
Дата публикации онлайн: 10.02.2022
Дата печати: 23.06.2022

List of abbreviations
MPM – multi-photon microscopy
PL – photoluminescence
PSF – point spread function
UCNP – upconversion nanoparticle
TCSPC – time-correlated single-photon counting module

Optical imaging assisted by molecular-specific fluorescent labelling is one of the main tools of the life sciences, which is commonly implemented with fluorescent organic dyes [1]. However, many molecular fluorophores are susceptible to their biochemical surroundings, exhibit unwanted properties, such as broad photoluminescent (PL) emission spectra, transient (blinking) and irreversible (photobleaching) light-induced transitions to dark electronic states [2], which limit their applicability [3]. Photostability is critical in many applications, including stimulated emission depletion microscopy [4].

PL nanoparticles typically exhibit excellent photostability [5], narrow and tunable spectra, [6], mild cytotoxicity [7]. Upconversion nanoparticles (UCNPs) represent promising PL nanomaterials, which meet the stringent requirements for ultrahigh-sensitivity optical imaging [8]. The list of merits includes virtually unlimited photostability; unique photochemical structure enables "upconversion" of near-infrared excitation light (975 nm) of the modest intensity (1–100 W/cm^2) to the higher energy visible/near-infrared emission (450–850 nm), as shown in Fig. 1A [9]. In addition, the exceptionally long (sub-ms) PL lifetimes of UCNPs (Fig. 1B) allow the realisation of time-gated detection schemes that can completely suppress the residual back-scattered excitation light [10].

To achieve the maximum PL efficiency of UCNPs [9], the excitation laser beam is focussed and raster-scanned across a specimen acquiring an image pixel-by-pixel, as schematically shown in Fig. 2A. Since the UCNP PL lifetime (τ_{UC}) is exceptionally long measured in sub-milliseconds (Fig. 1B), it takes about 30 min to acquire an image sized 512×512 by dwelling at every pixel for several milliseconds [11]. If the pixel dwell time during the scan is less than τ_{UC}, the PL signal will persist while being recorded and appear stretched along the scan-axis [12]. The demand of the high excitation intensity and exceptionally τ_{UC} precludes *in vivo* imaging.

Later works [12] have demonstrated an approach to solve this problem, where the low excitation power was employed by using a femtosecond laser in a multiphoton imaging modality; and the fast scan speed was determined by the same pixel dwell time as during traditional multiphoton imaging (about 10 μs). To remove the streaking, C.F. Gainer et al. [12] have proposed to apply a deconvolution procedure to the blurred

images. This approach was refined by D.V. Pominova et al. [13], where the authors reported the evaluation of τ_{UC}. Even though the application of the deconvolution procedure allowed visualising UCNPs with a resolution close to the diffraction limit, the proposed method had several shortcomings. The femtosecond laser tuned to 975 nm excited endogenous fluorescence alongside the excitation of UCNPs, and hence the image contrast was compromised. Continuous-mode laser excitation can improve the contrast [14], as well as the use of UCNP of the formula β-$NaYF_4$:Yb^{3+}, Tm^{3+}/$NaYF_4$ with the enhanced conversion efficiency (η_{UC}) [15]. These advances have the potential for image multiplexing and demultiplexing throughτ_{UC} [16], which can be

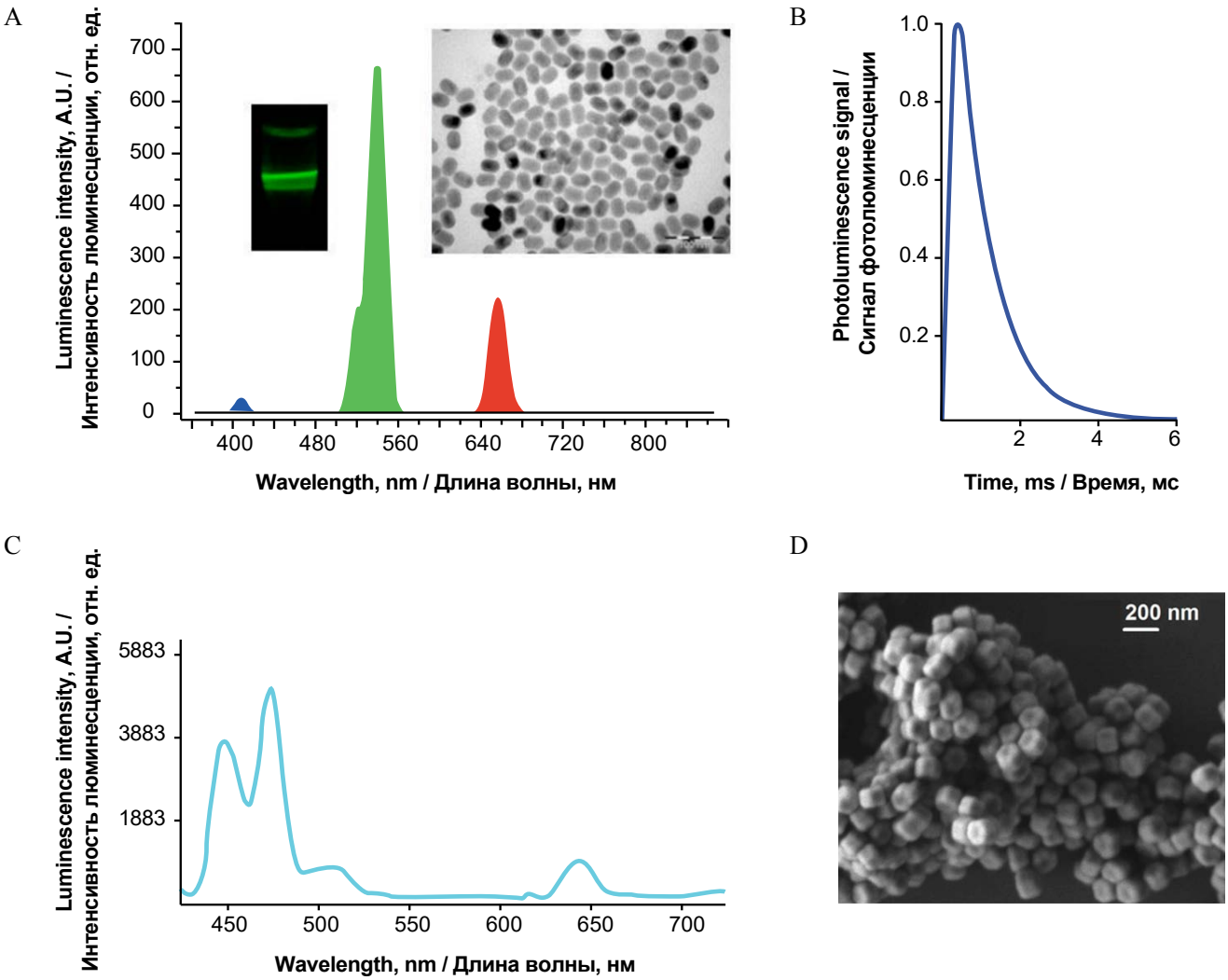

FIG. 1. Fluorescence characteristics and appearance of upconversion nanoparticles.
A. Photoluminescence spectrum and transmission electron microscopy image and photograph of colloidal UCNPs structured as $NaYF_4$:Yb: Er. The excitation laser at a wavelength of 975 nm was used to acquire the spectrum. An inset shows the photograph, where the laser path was visualised as a green strip, corresponding to the emission wavelengths at 522 nm, 541 nm.
B. A theoretically simulated plot of the PL signal versus time, PL lifetimeτ_{UC} = 0.8 ms was used as a parameter.
C. Spectra of the β-$NaYF_4$:Yb^{3+}, Tm^{3+}/$NaYF_4$ with 975-nm laser excitation.
D. Scanning electron microscopy images of β-$NaYF_4$: Yb^{3+}, Tm^{3+}/$NaYF_4$ T-UCNPs.

РИС. 1. Характеристики флуоресценции и внешний вид апконверсионных наночастиц.
A. Спектр фотолюминесценции, изображение с просвечивающего электронного микроскопа и фотография коллоидных UCNPs – $NaYF_4$:Yb:Er. Для получения спектра использовался возбуждающий лазер с длиной волны 975 нм. На вставке показана фотография, где путь лазера визуализирован в виде зеленой полосы, соответствующей длинам волн излучения 522 нм, 541 нм.
B. Теоретически смоделированный график зависимости сигнала PL от времени, время жизни PL UC = 0,8 мс.
C. Спектры β-$NaYF_4$:Yb^{3+},Tm^{3+}/$NaYF_4$ при лазерном возбуждении 975 нм.
D. Изображения со сканирующего электронного микроскопа β-$NaYF_4$: Yb^{3+},Tm^{3+}/$NaYF_4$ T-UCNPs.

Note: PL – photoluminescence, UCNPs – upconversion nanoparticles.
Примечание: PL – photoluminescence, фотолюминесценция, UCNPs – upconversion nanoparticles, апконверсионные частицы.

purpose engineered within a substantial tuning range from 1 to 2000 μs. The demultiplexing can be realised by the lifetime imaging using laser-scanning microscopy by dwelling over the UCNP-labelled regions for periods required to acquire the time trajectories sufficient to extract τ_{UC}. This method suffers from instrumental complexity and slow acquisition time.

We propose an approach, which relies on rapid raster-scanning of an UCNP-labelled specimen, while its persistent PL signal is continuously acquired from the entire scan area, as it is schematically presented in Fig. 2. The resultant blurred image can be reconstructed by performing an image post-processing procedure based on the image deconvolution with a temporal point-spread function of the single UCNP, where its τ_{UC} represents the key fitting parameter. As a result, the detection sensitivity of the PL signals was not compromised, despite the rapid pixel-by-pixel acquisition rate, and τ_{UC} was determined and can be used for image multiplexing/demultiplexing [16]. Although this approach has been described in Refs [12] and [13], the multiplexing/demultiplexing capability of this method has not been reported. Our study aimed to demonstrate the ability of the method to visualise two types of UCNPs in animal tissue.

MATERIALS AND METHODS

Synthesis of upconversion nanoparticles

We used two types of UCNPs of the structure $NaYF_4$:Yb:Er and $NaYF_4$:Yb:Er@$NaYF_4$, termed E1- and E2-UCNP, respectively. The synthesis of $NaYF_4$:Yb, Er@$NaYF_4$ nanoparticles was based on the Ostwald ripening-mediated method with some modification [17]. First, cubic $NaYF_4$ nanocrystals were prepared by mixing 1 mmol YCl_3, 6 mL oleic acid and 10 mL of octadecene in a 50-mL flask. The resulting mixture was heated to 150 °C under airflow under constant stirring for 30 min to form a light-yellow

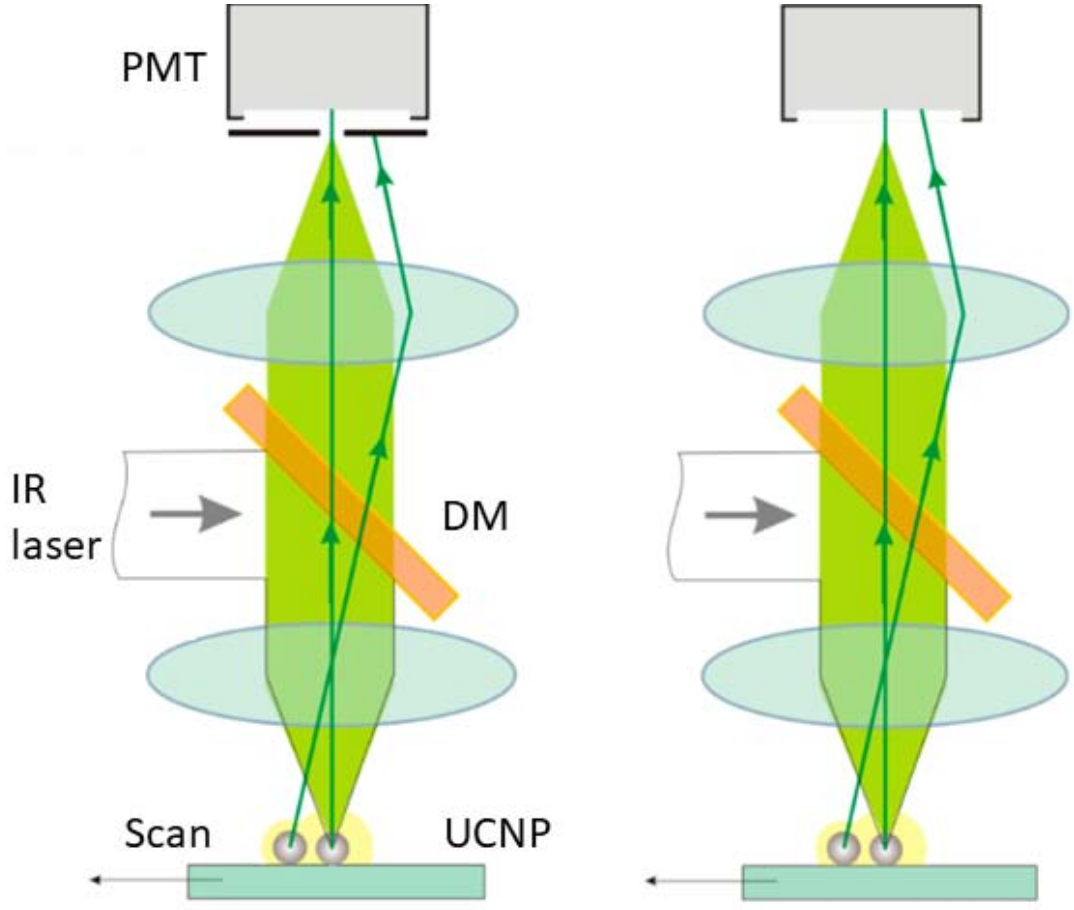

FIG. 2. Schematic diagram of a laser-scanning imaging system.
A near-infrared laser (IR laser) reflected off a dichroic mirror (DM) illuminates a sample containing discrete UCNPs and the sample is horizontally scanned. The emitted photoluminescence is detected by a photomultiplier (PMT).
РИС. 2. Схема системы лазерной сканирующей визуализации.
Луч лазера ближнего инфракрасного диапазона (IR laser), отраженный от дихроичного зеркала (DM), освещает образец, содержащий дискретные UCNPs. Образец сканируется в горизонтальном направлении. Излучаемая фотолюминесценция регистрируется фотоумножителем (PMT).

Note: UCNPs – upconversion nanoparticles.
Примечание: UCNPs – upconversion nanoparticles, апконверсионные частицы.

solution that was cooled down to room temperature. Then 10 mL of methanol solution with 1.6 mmol of NH_4F and 1 mmol of NaOH was added and stirred for 30 min. After heating to remove methanol, the solution was cooled. The solution was heated to 290 °C under argon flow using vigorous stirring for 45 min and cooled to room temperature. $NaYF_4$ nanoparticles obtained were collected and resuspended in a solution of 5-mL oleic acid, 8-mL octadecene. 0.2 mmol core UCNPs in 15-mL cyclohexane were added to a 100-mL flask, mixed with 10-mL oleic acid and 16 mL octadecene. The resultant core-shell $NaYF_4$:Yb, Er@$NaYF_4$ nanoparticles were collected and washed with centrifugation and dispersed in cyclohexane. Note that E1-UCNP is characterised by a much shorter emission lifetime in comparison with that of E2-UCNP.

Another type of UCNP, β-$NaYF_4$:Yb^{3+}, Tm^{3+}/$NaYF_4$, here termed T-UCNP, were synthesised using a procedure similar to that described above and reported in detail in [18].

Measurement of conversion coefficient of upconversion nanoparticles

The conversion coefficient of $NaYF_4$:Yb:Er @ $NaYF_4$ (η_{UC}) was evaluated to be about 2%. To improve it, we synthesised core-shell UCNP of the structure β-$NaYF_4$:Yb^{3+}, Tm^{3+}/$NaYF_4$ termed T-UCNP, as reported in detail in [17]. The conversion coefficient of T-UCNP was measured to be as high as 11% (Fig. 3B) and is much greater than ordinary two-photon absorption [13]. The distinct spectral bands of these particles are shown in the Fig. 1C.

The conversation efficiency of UCNPs is presented in Fig. 3B [17].

Animal experiments

All experiments with animals were performed using general anaesthesia (Zoletil mixture, 40 mg/kg of the animal's weight and 2% Rometar, 10 μL, 10 mg/kg) using intraperitoneal injection following the "Guide for the Care and Use of Laboratory Animals". The research was approved by the Ethics Committee of N.I. Lobachevsky State University of Nizhny Novgorod from 03.03.2021, protocol № 50. Two mice were housed in a single cage on a 12-h light/dark cycle under normal lighting conditions in transparent polycarbonate cages with an international standard stainless steel grid with ad libitum access to food and water using full-fat extruded feed for laboratory animals "Chara" and filtered ("Aquafor", Russia) water with complete replacement of water in drinking bottles 2 times a week.

Professional autoclavable material REHOFIX MK 2000 (granules from the core part of corn cobs) was used as bedding material, which was replaced every two days during the preparation and conduction of the experiment. Cleaning of the cages (washing the plastic base) was also performed once every two days. The air temperature was maintained within the range of 20–24 °C, with a relative humidity of 50 ± 20. To administer two types of UCNPs in live anaesthetised animals, we used 2 males at 8 weeks of age BALB/c mice weighing 20–25 *g* to examine the biodistribution of these particles after a single intravenous injection. The fur around the chest, abdomen and back areas of the animals was shaved to reduce scattering of the PL signal. 100 μL 0.05% wt. PA-UCNPs/PA colloidal solution (1 mg/kg) of phosphate buffer solutions, pH 7.2 was injected in a lateral tail vein. The detection of the PL was carried out on either the ventral or dorsal sides of the animals. The animals were euthanized 2 h after PA-UCNPs/PA injection by cervical spine dislocation. The liver was extracted and used for the imaging experiments.

RESULTS

Theoretical modelling

To demonstrate the advantages and limitations of the proposed lifetime imaging, we developed a simplified theoretical approach [15].

Consider a one-dimensional case of the laser-scanning PL imaging configuration, as shown in Fig. 2. A PL signal at the photomultiplier *S(t)* is modelled using the following expression:

$$S(t) \propto \int_{-\infty}^{t} dt' \Gamma(t') \int_{-\infty}^{\infty} dx G(x - vt') P(x), \quad (1)$$

G represents the intensity distribution of the excitation laser at 975 nm. G depends on the space and time variables, *x*, *t*, respectively, which are functionally dependent as *x–vt*, and describe a travelling wave propagating in the positive x-direction with the speed v. *P(x)* represents the UCNP sample profile. The UCNP PL versus time is described by *Γ(t)* [19], with the time trajectory shown in Fig. 1B. This time trajectory features the PL signal rise and is explained by the complex upconversion energy transfer processes. The second phase of decay is determined primarily by the UCNP PL lifetime τ_{ph}. Assume $\Gamma = e^{\frac{-t}{\tau_{ph}}}$, and a Gaussian function intensity distribution $(x - vt) = exp[-(\frac{x-vt}{2w})^2]$, with the beam waist, *w* equal to the focussed beam diameter.

Consider the sample as a discrete set of UCNPs with diameters << *w*. A single UCNP is modelled as a delta-function positioned at = 0, i.e. *P(x)*=δ(0). If τ_{ph} is comparable with the scanning time, i.e. $\tau_{ph} \sim \tau_s$ the expression (1) is transformed to:

$$S(t) \propto \int_{-\infty}^{t} dt' \, exp \, exp\left(\frac{t'-t}{\tau_{ph}}\right) exp[-\frac{1}{2}(\frac{vt'}{w})^2] \propto$$

$$\propto \frac{e^{\frac{-t}{\tau_{ph}}}}{2}\left\{1 + erf\left[\frac{v}{\sqrt{2}w}\left(t - \frac{w^2}{v^2\tau_{ph}}\right)\right]\right\}, \quad (2)$$

where erf – the error function, where (x_i, y_i) – T-UCNP coordinates, A_i – the relative amplitude of the signal. Evaluation of the expression (2) leads to the conclusion that this is a convolution of the surface profile of UCNP with the time-decay function of UCNP, i.e. temporary function Γ(t). One can think of *S* as the impulse function, which can be used for deconvolution, where two parameters need to be adjusted for the best results: τ_{ph} and w. PL signal can be acquired by rapidly scanning through the sample, and the surface distribution of UCNP is reconstructed at the

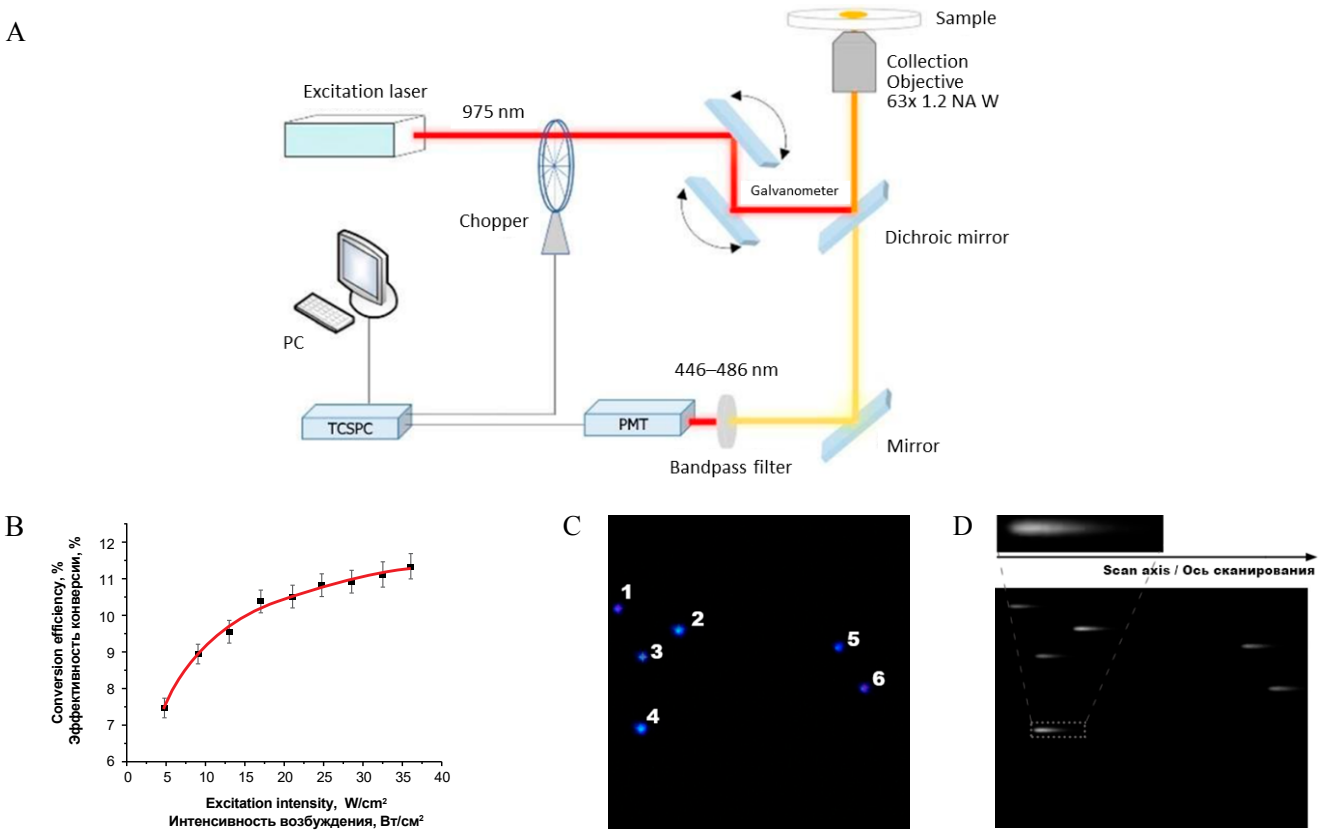

FIG. 3. Setup for obtaining photoluminescence spectra, photoluminescence lifetime and imaging. Results obtained with this system.
A. Schematic of the setup for the acquisition of the PL emission time trajectories of UCNP:β-$NaYF_4$:Yb^{3+}, Tm^{3+}/$NaYF_4$.
B. Plot of the integral conversion coefficient of UCNPs as a function of the excitation intensity at 975 nm measured using an integrating sphere. The PL saturation was achieved at ~20 W cm-2.
C. Image of T-UCNP discrete particles on a coverslip obtained in wavelength-scan mode. The image size, 137 mm×137 mm. Numbers 1–6 indicate individual UCNPs.
D. T-UCNP images were obtained using a laser-scanning multiphoton microscopy setup with a laser beam pixel Dwell Time of 12.61 μs.
РИС. 3. Установка для получения спектров фотолюминесценции, времени жизни фотолюминесценции и визуализации. Результаты, полученные с помощью этой системы.
A. Схема установки для получения временных траекторий PL-эмиссии UCNP:β-$NaYF_4$:Yb^{3+},Tm^{3+}/$NaYF_4$.
B. График интегрального коэффициента конверсии UCNP в зависимости от интенсивности возбуждения при 975 нм, измеренный с помощью интегрирующей сферы. Насыщение ФЛ было достигнуто при ~20 Вт $см^{-2}$.
C. Изображение дискретных частиц T-UCNP на покровном стекле, полученное в режиме сканирования по длине волны. Размер изображения 137×137 мм. Цифрами 1–6 обозначены отдельные UCNP.
D. Изображения T-UCNP, полученные с помощью установки многофотонной микроскопии с лазерным сканированием и временем пребывания пикселя лазерного луча 12,61 мкс.

Note: PL – photoluminescence, UCNP – upconversion nanoparticle, PMT – photomultiplier, TCSPC – time-correlated single photon counting.
Примечание: PL – photoluminescence, фотолюминесценция, UCNP – upconversion nanoparticle, апконверсионная частица, PMT – photomultiplier, фотоумножитель, TCSPC – time correlated single photon counting, счет одиночных фотонов с корреляцией по времени.

post-processing stage. It was straightforward to generalise the 1D-case to 2D-case.

The theoretical modelling of single-particle T-UCNP was carried out using the following formula, where *vt* is replaced by the time-dependent coordinate *x*:

$$S(x,y) \propto \frac{1}{2}\sum_{i=1}^{N} A_i exp\left[-\frac{(y-y_i)^2}{2w^2}\right] exp\left[\frac{x_i-x}{v\tau_{ph}}\right]\{1+ \\ + erf\left[\frac{x-x_i}{\sqrt{2}w}\right]\} + Noise \quad (3)$$

Where (x_i,y_i) is T-UCNP coordinates, A_i – is the relative amplitude of the signal.

To restore an undistorted T-UCNP image, we used the Lucy – Richardson algorithm. Fig. 4 (right panel) represents an image processed using the Lucy – Richardson algorithm, in which expression (3) was used as the point spread function (PSF) input function under the summation sign.

Deconvolution of discrete upconversion nanoparticles with known τ

The result of the numerical simulation of a 2D PL image of a set of UCNPs randomly distributed in the field of view is shown in Fig. 4A randomly distributed noise was also

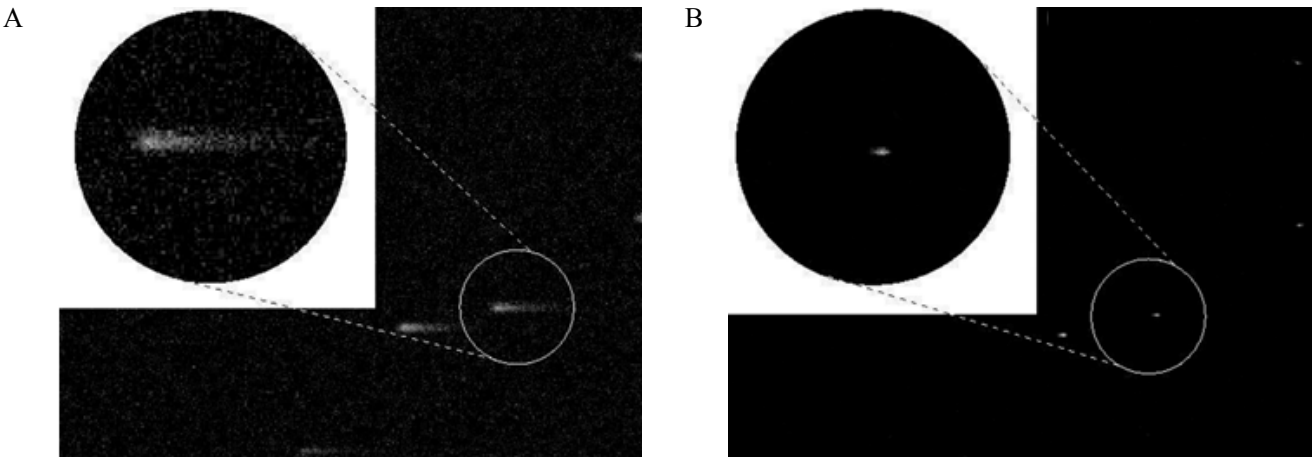

FIG. 4. A 2D photoluminescence image of a set of upconversion nanoparticles simulated numerically.
Insets show zoomed-in images of the areas demarcated by white-colour circles.
A. Original image. B. Reconstructed image.
РИС. 4. Двумерное фотолюминесцентное изображение набора апконверсионных наночастиц, смоделированных численно.
Вставки показывают увеличенные изображения областей, выделенных кружками белого цвета.
А. Исходное изображение. В. Реконструированное изображение.

added to test the robustness of the image reconstructions procedure. Note the significant reduction of the original image size. We emphasis a significant improvement of the signal-to-noise ratio evident by visual examination of the salt-and-pepper noise (Fig. 4A). This noise is unobservable in the reconstructed image (Fig. 4B).

Rapid image acquisition was realised by setting the excitation intensity to a value higher than the saturation power density of E2-UCNPs (>0.1 Jcm^{-2}) easily achievable at the typical settings of the laser-scanning microscope. The focussed laser beam was scanned at a speed of 10 cm/s and dwelled about 10 μs at each pixel. The specimen represented a thin slice of the liver tissue extracted from a mouse 3-h post-injection of E2-UCNPs prepared in phosphate buffer saline. Fig. 5A shows an overlay of the bright-field image of the liver tissue and PL image of E2-UCNPs accumulated in this tissue. Comet-like PL signals from single or clustered UCNPs are readily observable. Fig. 5B presents these signals as a surface plot. The image deconvolution procedure was applied, and the result is presented in Fig. 5C. The blurred PL image was converted into a set of intense narrow discrete peaks of about 1.5-μm in diameter comparable to the diffraction-limited spots. The E2-UCNP PL lifetime was determined to be 0.8 ms in good agreement with the expected value (Fig. 1B).

T-UCNP photoluminescence kinetics measurements

PL lifetime of UCNPs (τ_{ph}) represents an important configuration parameter for the deconvolution procedure. We measured τ_{ph} using an alternative method employing a setup equipped with an optical modulator (chopper) and time-correlated single-photon counting module (TCSPC) by processing images of the sample scan. For each particle shown in Fig. 3C, PL attenuation curves in the spectral range of 446–486 nm were recorded using the scheme shown in Fig. 3A. The obtained curves were approximated by a dependence of the form

$$f(t) = a_1 e^{-\frac{t}{\tau_1}} + a_2 e^{-\frac{t}{\tau_2}}, \quad (4)$$

with the lifetimes of the exponential components τ, and the amplitudes of the exponential components *a*.

The parameters τ_m and t_i were calculated to determine the average lifetime of the studied T-UCNP:

τ_m – the average lifetime of the components of a multi-exponential decay weighted by their amplitude coefficients (a_1,$a_2$etc.). For a two-exponential decay, τ_m is defined as expression (5):

$$\tau_m = a_1\tau_1 + a_2\tau_2;\ a_1 + a_2 = 1. \quad (5)$$

t_i – the average lifetime of the decreasing components weighted by their integral intensities. The intensity-weighted value of t_i for a two-exponential decay is defined as expression (6):

$$t_i = \frac{a_1\tau_1^2 + a_2\tau_2^2}{a_1\tau_1 + a_2\tau_2}, \quad (6)$$

The mean lifetime t_i is more sensitive to changes in the slow component of the lifetime, while the mean lifetime τ_m is more sensitive to changes in the fast component.

Then, without changing the position of the sample, the sample was scanned at the scanning speed corresponding to the pixel dwell value of 12.61 μs. The resulting image is shown in Fig. 3D.

The PL signal profile of each particle was extracted for subsequent deconvolution using the view function [expression (6)]:

$$I = Aexp\left(\frac{t_0 - t}{\tau_1}\right) - Bexp\left(\frac{t_0 - t}{\tau_2}\right) + C, \quad (7)$$

where I is the intensity of the nanoparticle's PL signal; t_0 and t are the sample scanning time (t_0) is the time

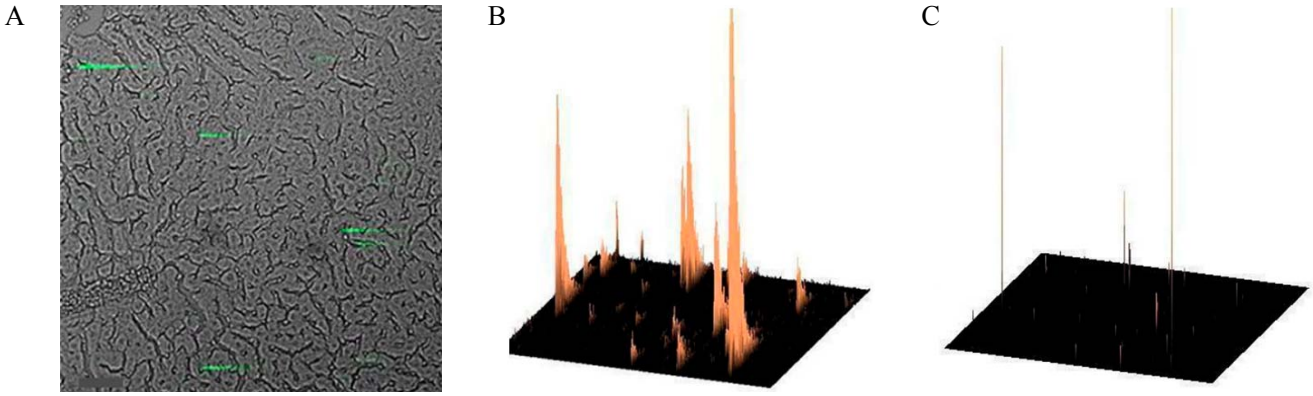

FIG. 5. Deconvolution of the blurred image of upconversion nanoparticles in a mouse liver tissue sample.
A. An overlaid bright-field image of the mouse liver tissue (grey) and PL image of E2-UCNPs (green) deposited in the liver post-intravenous injection. Scale bar, 50 μm.
B. Surface plot of originally acquired and
C. deconvolved PL images of UCNPs in the liver slice, as in (A).
РИС. 5. Деконволюция размытого изображения апконверсионных наночастиц в образце ткани печени мыши.
A. Наложенное ярко-полевое изображение ткани печени мыши (серый) и PL изображение E2-UCNPs (зеленый), осажденных в печени после внутривенной инъекции. Масштаб – 50 мкм.
B. Поверхностный график изначально полученного изображения PL UCNP (A).
C. Поверхностный график изображения PL UCNP (A) после процедуры деконволюции.

Note: PL – photoluminescence, UCNPs – upconversion nanoparticles.
Примечание: PL – photoluminescence, фотолюминесценция, UCNPs – upconversion nanoparticles, апконверсионные частицы.

corresponding to the moment of the beginning of PL signal growth when the scanner passes through the sample area in which the particle is located); since the PL signal profile obtained from the microscope is a dependence of the PL signal on the scanner position (in pixels), to convert the abscissa scale from x (pixels) to t (μs), the initial values of x were multiplied by the scanning time of one pixel (Pixel Dwell); τ_1 – parameter corresponding to the UCNP PL signal decline time; τ_2 – parameter corresponding to the T-UCNP PL signal rise time; A and B – amplitude factors; C – the background signal value (noise level).

1. The value of τ_2 was chosen as the value corresponding to the time during which the PL signal increases by approximately 1/3 of the intensity at the maximum;

2. t_0 was fixed as a value of time corresponding to the moment of the beginning of the growth of the UCNP signal.

τ_{ph} of T-UCNP measured by the multi-photon microscopy (MPM) method, as well as τ_m and t_i values obtained using TCSPC, are shown in Fig. 6.

One can see that the deconvolution method provides an underestimate of τ_{UC} in comparison with the more reliable method based on the chopper/TCSPC module.

Lifetime imaging using multiplexing/demultiplexing from two types of upconversion nanoparticles

To demonstrate the capability of multiplexing/demultiplexing, we carried out lifetime imaging using 2 types of UCNPs embedded in excised animal tissue. As the long and short emission lifetime UCNPs we selected T- and E1-UCNPs, respectively. A cocktail of UCNPs was administered in a live laboratory animal, and the extracted liver was sliced and examined (see M&M for details). Fig. 7A shows a photograph of a mouse liver containing two types of particles, obtained using a raster scan with a long dwell time in the laser beam per pixel (177 μs). By measuring the PL spectra of each pixel as shown in Fig. 7C by measurements

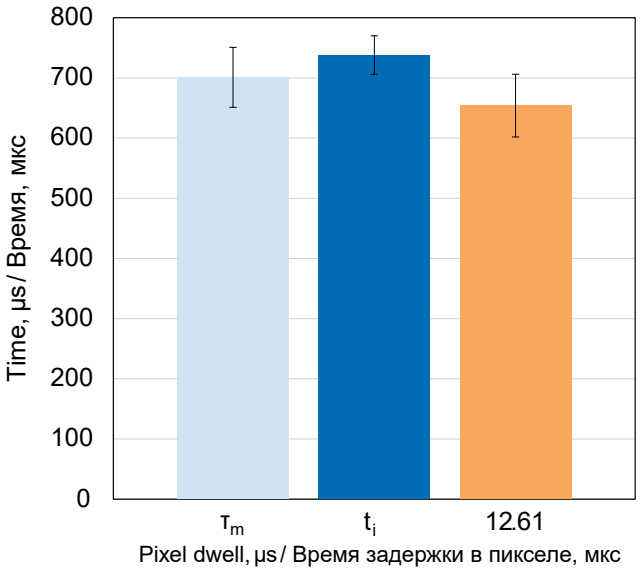

FIG. 6. Comparison of the photoluminescence lifetimes of T-UCNPs in the 446–486 nm range obtained by different methods.
РИС. 6. Сравнение времени жизни фотолюминесценции T-UCNPs в диапазоне 446–486 нм, полученное различными методами.

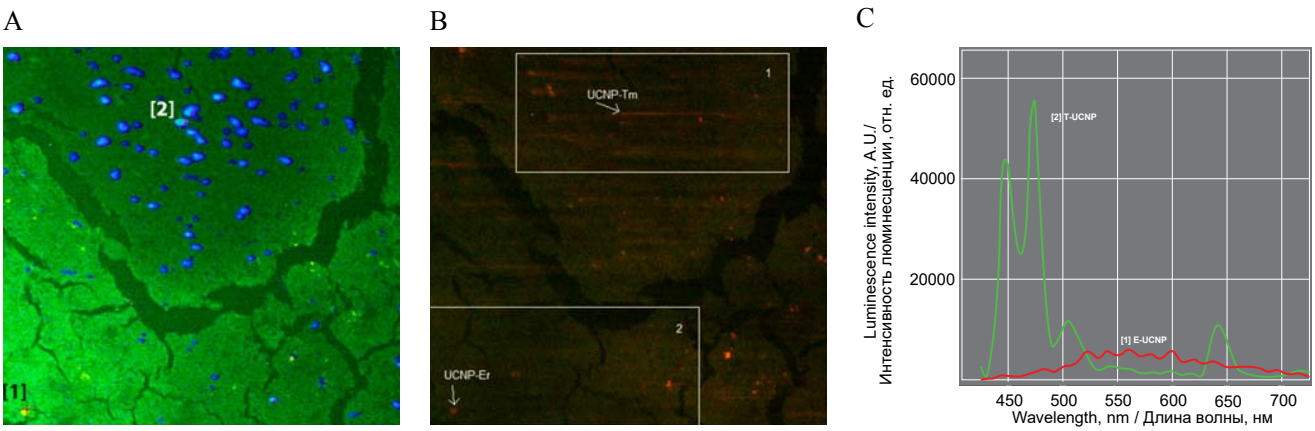

FIG. 7. Experiments with a mouse liver slice containing two types of particles.
A. A multiphoton microscopy image of the mouse liver slice containing T- (blue) and E1- (yellow) UCNPs acquired by raster scanning with the fully open aperture, image size 424×424 μm, Pixel Dwell: 177 μs.
B. T-UCNP (denoted UCNP-Tm) shows a pronounced streak pattern, whereas E1-UCNP (denoted UCNP-Er) shows almost unobservable streaking.
C. Particle PL spectra taken at points [1] and [2] marked in Fig. 7A. Fast scanned MPM image of the same sample, image size 424×424 μm, Pixel Dwell: 12.6 μs.
РИС. 7. Эксперименты со срезом печени мыши, содержащим два типа частиц.
A. Мультифотонное микроскопическое изображение среза печени мыши, содержащего T- (синий) и E1- (желтый) UCNPs, полученное методом растрового сканирования с полностью открытой диафрагмой, размер изображения 424×424 мкм, Pixel Dwell: 177 мкс.
B. T-UCNP (обозначено UCNP-Tm) демонстрирует ярко выраженный полосатый рисунок, тогда как E1-UCNP (обозначено UCNP-Er) демонстрирует почти ненаблюдаемое размытие.
C. Спектры PL частиц, снятые в точках (1) и (2), отмеченных на рис. 7A. Быстрое сканирование MPM изображения того же образца, размер изображения 424×424 мкм, Pixel Dwell: 12,6 мкс.

Note: MPM – multi-photon microscopy, PL – photoluminescence, UCNP – upconversion nanoparticle.
Примечание: MPM – multi-photon microscopy, многофотонная микроскопия, PL – photoluminescence, фотолюминесценция, UCNP – upconversion nanoparticle, апконверсионная частица.

at points (1) and (2) of Fig. 7A, we were able to identify T- and E1-UCNPs, since the PL spectrum of the T-UCNP particles was distinguished by pronounced peaks in the 450–508 nm (blue) region, whereas E1-UCNP featured characteristic spectral bands in green and red.

Next, the same sample was scanned using the MPM system (Fig. 7B). In the region where we were able to identify T-UCNP from the previous experiment, we observed a blurring of the point in a line along the scan-axis, which was absent in the region where the short-lived E1-UCNP was located. This was due to the much longer lifetime of T-UCNP compared to E1-UCNP. Thus, it became possible to distinguish, identify particles in the sample by the character of the observed comet-like blurring of the point. Besides, τ_{UC} can be evaluated.

DISCUSSION

We demonstrated a method to rapidly acquire images of discrete photoluminescent nanomaterials by operating a commercial nonlinear optical microscopy in a non-descanned detection mode. The resultant blurred patterns produced by discrete PL nanoparticles such as UCNPs were processed by a deconvolution algorithm to achieve an almost diffraction-limited PSF. Besides, we demonstrated the reconstruction of τ_{ph}. Since it is possible to engineer τ_{ph} of UCNP, we produced 2 types of UCNP with long and short τ_{ph} to demonstrate multiplexing and demultiplexing to identify both types of UCNPs. This capacity was useful to discriminate different UCNPs in turbid biological tissue [16].

Among the shortcomings of the reported method, the accuracy of determination of τ_{UC} is limited by the signal-to-noise ratio – the method tends to underestimate τ_{ph}, as it was the case shown in Fig. 3D. Secondly, the increased excitation intensity leads to the broadening of PSF of UCNPs and can compromise the resolution. For example, Fig. 7 shows discrete nanoparticles sized several micrometres in diameter. This limitation can be circumvented by using unique types of T-UCNP [20], but this limits the repertoire of available PL nanomaterials. Thirdly, the multiplexing capacity is limited by the image size and laser-scanning rate, which can accommodate the longest τ_{ph}, while the shortest τ_{ph} may remain undetectable. This scenario is demonstrated in Fig. 7B, where E1-UCNP featuring short τ_{ph} showed negligible streaking, while T-UCNP showed the streaking of the length comparable with the image size.

CONCLUSION

In this communication, we demonstrated a new approach for rapid PL (phosphorescence) image acquisition of samples containing PL materials,

such as biological specimens labelled with discrete UCNPs using laser scanning multiphoton microscopy. The comet-like blurred images of discrete UCNPs obtained as a result of the rapid scanning were reconstructed by applying the deconvolution procedure. The contrast of discrete UCNP images was enhanced, and the UCNP emission lifetimes were determined. This enabled demonstration of multiplexing/demultiplexing using lifetime imaging mode, where the UCNP lifetime was engineered. The power of this method was demonstrated by the identification of 2 types of UCNPs accumulated in the liver of a laboratory animal. We believe that the demonstrated method can be useful for rapid lifetime imaging where several molecular specific labelling agents are required.

AUTHOR CONTRIBUTION

Andrey V. Yudintsev carried out experiments, Artyom O. Zviagintcev and Alireza Maleki implemented image reconstruction algorithms, Vladimir A. Vodeneev developed the signal processing and image reconstruction algorithms, Andrei V. Zvyagin conceived the main concept, coordinated the project and took part in writing the manuscript together with Artyom O. Zviagintcev and Alireza Maleki. All authors participated in the discussion and editing of the work. All authors approved the final version of the publication.

ВКЛАД АВТОРОВ

А.В. Юдинцев провел эксперименты, А.О. Звягинцев и Малеки Алиреза реализовали алгоритмы восстановления изображений, В.А. Воденеев разработал алгоритмы обработки сигналов и реконструкции изображений, А.В. Звягин разработал основную концепцию, координировал проект и участвовал в написании рукописи вместе с А.О. Звягинцевым и Малеки Алирезой. Все авторы участвовали в обсуждении и редактировании работы. Все авторы одобрили окончательную версию публикации.

SUPPLEMENTARY MATERIALS

Supplementary materials associated with this article can be found in the online version at doi: https://doi.org/10.47093/2218-7332.2022.338.06.S

ДОПОЛНИТЕЛЬНЫЕ МАТЕРИАЛЫ

Дополнительные материалы, прилагаемые к этой статье, можно посмотреть в онлайн-версии по адресу: https://doi.org/10.47093/2218-7332.2022.338.06.S

REFERENCES / ЛИТЕРАТУРА

1 *Moerner W.E.* New directions in single-molecule imaging and analysis. Proc Natl Acad Sci U S A. 2007 Jul 31; 104 (31): 12596–602. https://doi.org/10.1073/pnas.0610081104. Epub 2007 Jul 30. Erratum in: Proc Natl Acad Sci U S A. 2007 Sep 25; 104 (39): 15584. PMID: 17664434.

2 *Gómez D.E., van Embden J., Jasieniak J., et al.* Blinking and surface chemistry of single CdSe nanocrystals. Small. 2006 Feb; 2(2): 204–8. https://doi.org/10.1002/smll.200500204. PMID: 17193021.

3 *Altman R.B., Terry D.S., Zhou Z., et al.* Cyanine fluorophore derivatives with enhanced photostability. Nat Methods. 2011 Nov 13; 9(1): 68–71. https://doi.org/10.1038/nmeth.1774. PMID: 22081126.

4 *Hell S.W.* Far-field optical nanoscopy. Science. 2007 May 25; 316 (5828): 1153–8. https://doi.org/10.1126/science.1137395. PMID: 17525330.

5 *Sreenivasan V.K., Zvyagin A.V., Goldys E.M.* Luminescent nanoparticles and their applications in the life sciences. J Phys Condens Matter. 2013 May 15; 25(19): 194101. https://doi.org/10.1088/0953-8984/25/19/194101. Epub 2013 Apr 24. PMID: 23611923.

6 *Edmonds A.M., Sobhan M.A., Sreenivasan V.K., et al.* Nano-ruby: a promising fluorescent probe for background-free cellular imaging. Particle & Particle Systems Characterization. 2013; 30(6): 506–13. https://doi.org/10.1002/ppsc.201200112.

7 *Yu S.J., Kang M.W., Chang H.C., et al.* Bright fluorescent nanodiamonds: no photobleaching and low cytotoxicity. J Am Chem Soc. 2005 Dec 21; 127(50): 17604–5. https://doi.org/10.1021/ja0567081. PMID: 16351080.

8 *Yuan J., Wang G.* Lanthanide-based luminescence probes and time-resolved luminescence bioassays. TrAC Trends in Analytical Chemistry. 2006; 25(5): 490–500. https://doi.org/10.1016/j.trac.2005.11.013.

9 *Nadort A., Sreenivasan V.K., Song Z., et al.* Quantitative imaging of single upconversion nanoparticles in biological tissue. PLoS One. 2013 May 14; 8(5): e63292. https://doi.org/10.1371/journal.pone.0063292. PMID: 23691012.

10 *Zhan Q., He S., Qian J., et al.* Optimization of optical excitation of upconversion nanoparticles for rapid microscopy and deeper tissue imaging with higher quantum yield. Theranostics. 2013. Mar 23; 3(5): 306–16. https://doi.org/10.7150/thno.6007. PMID: 23650478.

11 *Wu S., Han G., Milliron D.J., et al.* Non-blinking and photostable upconverted luminescence from single lanthanide-doped nanocrystals. Proc Natl Acad Sci U S A. 2009 Jul 7; 106(27): 10917–21. https://doi.org/10.1073/pnas.0904792106. Epub 2009 Jun 18. PMID: 19541601.

12 *Gainer C.F., Utzinger U., Romanowski M.* Scanning two-photon microscopy with upconverting lanthanide nanoparticles via Richardson-Lucy deconvolution. J Biomed Opt. 2012 Jul; 17(7): 076003. https://doi.org/10.1117/1.JBO.17.7.076003. PMID: 22894486.

13 *Pominova D.V., Ryabova A.V., Grachev P.V., et al.* Upconversion microparticles as time-resolved luminescent probes for multiphoton microscopy: desired signal extraction from the streaking effect. J Biomed Opt. 2016 Sep 1; 21(9): 96002. https://doi.org/10.1117/1.JBO.21.9.096002. PMID: 27604561.

14 *Kostyuk A.B., Guryev E.L., Vorotnov A.D., et al.* Real-Time Tracking of Yb3+, Tm3+ Doped NaYF4 Nanoparticles in Living Cancer Cells. Sovremennye tehnologii v medicine 2018; 10(1): 57–63. http://doi.org/10.17691/stm2018.10.1.07.

15 *Kostyuk A.B., Vorotnov A.D., Ivanov A.V., et al.* Resolution and contrast enhancement of laser-scanning multiphoton microscopy using thulium-doped upconversion nanoparticles. Nano Res. 2019; 12: 2933–40. https://doi.org/10.1007/s12274-019-2527-0.

16 *Fan Y., Wang P., Lu Y., et al.* Lifetime-engineered NIR-II nanoparticles unlock multiplexed in vivo imaging. Nat Nanotechnol. 2018 Oct; 13(10): 941–6. https://doi.org/10.1038/s41565-018-0221-0. Epub 2018 Aug 6. PMID: 30082923.

17 *Johnson N.J., Korinek A., Dong C., van Veggel F.C.* Self-focusing by Ostwald ripening: a strategy for layer-by-layer epitaxial growth on upconverting nanocrystals. J Am Chem Soc. 2012 Jul

11; 134(27): 11068–71. https://doi.org/10.1021/ja302717u. Epub 2012 Jun 26. PMID: 22734596.

18 *Rocheva V.V., Koroleva A.V., Savelyev A.G., et al.* High-resolution 3D photopolymerization assisted by upconversion nanoparticles for rapid prototyping applications. Sci Rep. 2018 Feb 26; 8(1): 3663. https://doi.org/10.1038/s41598-018-21793-0. PMID: 29483519.

19 *Hehlen M., Kuditcher A., Lenef A., et al.* Nonradiative dynamics of avalanche upconversion in Tm: LiYF4. Physical Review B. 2000; 61(2): 1116. https://doi.org/10.1103/PhysRevB.61.1116

20 *Zhao J., Jin D., Schartner E.P., et al.* Single-nanocrystal sensitivity achieved by enhanced upconversion luminescence. Nat Nanotechnol. 2013 Oct; 8(10): 729–734. https://doi.org/10.1038/nnano.2013.171. Epub 2013 Sep 1. PMID: 23995455.

INFORMATION ABOUT THE AUTHORS / ИНФОРМАЦИЯ ОБ АВТОРАХ

Artyom O. Zviagintcev, student intern, Federal Scientific Research Centre "Crystallography and Photonics" of Russian Academy of Sciences.
ORCID: https://orcid.org/0000-0002-4490-4867

Andrey V. Yudintsev, Cand. of Sci. (Phys. and Math.), Associate Professor, Lecturer of the Department of Biophysics, Institute of Biology and Biomedicine, Lobachevsky Nizhny Novgorod State University.
ORCID: https://orcid.org/0000-0003-0333-5095

Alireza Maleki, Postdoctoral Research Fellow, Department of Physics and Astronomy, Macquarie University, Australia.
ORCID: https://orcid.org/0000-0003-2852-2102

Vladimir A. Vodeneev, Dr. of Sci. (Biology), Associate Professor, Head of the Department of Biophysics, Institute of Biology and Biomedicine, Lobachevsky Nizhny Novgorod State University.
ORCID: https://orcid.org/0000-0002-3726-5577

Andrei V. Zvyagin✉, Dr. of Sci. (Phys. and Math.), Institute of Biology and Biomedicine, Lobachevsky Nizhny Novgorod State University; Biomedical Physics Group, Head Faculty of Science and Engineering, Macquarie University, Australia.
ORCID: https://orcid.org/0000-0001-8799-2257

Звягинцев Артём Олегович, студент-стажер ФНИЦ «Кристаллография и фотоника» РАН.
ORCID: https://orcid.org/0000-0002-4490-4867

Юдинцев Андрей Владимирович, канд. физ.-мат. наук, доцент, преподаватель кафедры биофизики Института биологии и биомедицины ФГАУ ВО «Национальный исследовательский Нижегородский государственный университет им. Н.И. Лобачевского».
ORCID: https://orcid.org/0000-0003-0333-5095

Малеки Алиреза, аспирант-исследователь факультета физики и астрономии Университета Маккуори, Австралия.
ORCID: https://orcid.org/0000-0003-2852-2102

Воденеев Владимир Анатольевич, д-р биол. наук, доцент, заведующий кафедрой биофизики Института биологии и биомедицины ФГАУ ВО «Национальный исследовательский Нижегородский государственный университет им. Н.И. Лобачевского».
ORCID: https://orcid.org/0000-0002-3726-5577

Звягин Андрей Васильевич✉, д-р физ.-мат. наук, Институт биологии и биомедицины ФГАУ ВО «Национальный исследовательский Нижегородский государственный университет им. Н.И. Лобачевского»; группа биомедицинской физики, руководитель факультета науки и техники Университета Маккуори, Австралия.
ORCID: https://orcid.org/0000-0001-8799-2257

✉ Corresponding author / Автор, ответственный за переписку